Ecological Engineering & Environmental Technology, 2025, 26(12), 212–225 https://doi.org/10.12912/27197050/214122 ISSN 2719–7050, License CC-BY 4.0

Quantifying annual mangrove forest gross primary productivity in Bali for blue carbon management

I Wayan Nuarsa^{1,2}, Abd. Rahman As-syakur², Moh Saifulloh², Herlambang Aulia Rachman³, I Kade Alfian Kusuma Wirayuda⁴

- ¹ Environmental Science Doctoral Program, Postgraduate, Udayana University, Denpasar, Department of Marine Sciences, Trunojoyo University of Madura, Indonesia
- ² Marine Science Study Program, Faculty of Marine and Fisheries, Udayana University, Jimbaran, Indonesia
- ³ Department of Marine Sciences, Trunojoyo University of Madura, Indonesia
- ⁴ Aquatic Resource Management Study Program, Faculty of Marine and Fisheries, Udayana University, Jimbaran, Indonesia
- * Corresponding author's e-mail: m.saifulloh@unud.ac.id

ABSTRACT

This research quantified the annual gross primary productivity (GPP) dynamics of Bali's two largest mangrove areas, the Ngurah Rai Grand Forest Park (Tahura Ngurah Rai) and the West Bali National Park (TNBB), from 2019 to 2024. Using the Vegetation Photosynthesis Model (VPM) in Google Earth Engine with Sentinel-2A, MODIS LST, and ERA5 data, we produced a high-resolution carbon assimilation baseline. The findings reveal a strengthening photosynthetic uptake, with a province-wide mean GPP near 3.6 kg C m² yr¹ and a peak in 2023. Site-level productivity increased by 11.0% at Tahura Ngurah Rai and 7.4% at TNBB. Spatially, GPP diverged significantly: interior, protected canopies were highly productive (averaging > 4.3 kg C m² yr¹) and stable, whereas disturbed edge zones, such as near the Suwung landfill in Tahura Ngurah Rai, exhibited low GPP (mean 2.7 kg C m² yr¹) and high variability (12.8% CV). These results highlight clear management priorities: preserving high-GPP interior stands and restoring vulnerable edge zones. This high-resolution monitoring provides an actionable baseline for Bali's blue carbon strategies, contributing critical data on ecosystem function for a globally significant tourist and ecological region.

Keywords: mangrove, blue carbon, vegetation photosynthesis model, carbon assimilation, light use efficiency, spatial dynamics, ecosystem services, mangrove management.

INTRODUCTION

Indonesia has committed to achieving Net Zero Emissions by 2060, with an interim plan to reduce emissions by 834 million tons CO₂ or 29% relative to a business-as-usual scenario by 2030. By 2018, national mitigation actions had already delivered a 7.55% reduction through improved sustainable land management and increases in tree cover (UNFCCC, 2022). The national forest area in 2020 was reported at 95.6 million hectares, equivalent to 50.9% of land area, including an estimated 3.31 million hectares of mangroves with substantial potential for carbon uptake and storage (Government of Indonesia, 2022).

Mangrove ecosystems are among the most efficient natural systems for sequestering and storing carbon. Although they occupy relatively small coastal zones, their carbon stocks can exceed those of many terrestrial forests. Mangrove deforestation, estimated at 0.7% of total forest area, has been associated with emissions of 0.02 to 0.12 pg of carbon per year, which is roughly 10% of global deforestation emissions (Donato et al., 2011; McLeod et al., 2011). Understanding the short-term and interannual behaviour of carbon uptake is therefore critical. Gross primary productivity (GPP) measures the total carbon fixed through photosynthesis over a given period and is a central indicator for evaluating the efficiency of

Received: 2025.11.10

Accepted: 2025.11.15

Published: 2025.12.01

vegetation in assimilating atmospheric CO₂ (Running et al., 2004; Zhao et al., 2005).

Bali Province faces notable environmental pressure due to rapid population growth and urban expansion associated with tourism. The provincial population reached 4.32 million in 2020 with a density of 747 people per square km, up from 673 people per km² in 2010, with an absolute increase of approximately 348,000 people between 2013 and 2023 (Badan Pusat Statistik, 2024). Land conversion from vegetated surfaces to built-up areas for tourism infrastructure reduces the capacity of terrestrial landscapes to absorb carbon. This context elevates the strategic importance of mangrove ecosystems in provincial climate mitigation and coastal management.

Satellite remote sensing provides spatially and temporally consistent observations for tracking land-cover change and vegetation productivity (Nuarsa, 2016; Nuarsa et al., 2015). Vegetation indices such as the enhanced vegetation index (EVI) and the land surface water index (LSWI) are widely used as inputs to light-use-efficiency frameworks, including the Vegetation Photosynthesis Model, to estimate GPP as a proxy for photosynthetic carbon uptake (Xiao et al., 2010; Xiao et al., 2004). In Bali's urban context, previous studies reported a decline in total terrestrial GPP of 7,793.96 tC per year, or 12.65%, over 1995 to 2014, linked to urbanization driven by tourism (Nuarsa et al., 2018). In contrast, within Sanur from 2006 to 2015, green open spaces increased GPP by 26% despite development pressure (As-syakur et al., 2023). For mangroves near Benoa Port, GPP reportedly declined from 28.790 tC per year in 2016 to 26.223 tC per year in 2020, likely reflecting land-cover change and development pressures (Romadhoni et al., 2022). Other work in Tahura Ngurah Rai has focused on total carbon stocks rather than photosynthetic uptake, using both satellite data and field measurements (Hidayah et al., 2024; Suardana et al., 2023; Sugiana et al., 2024). Collectively, these studies underscore the sensitivity of productivity to urbanization and management, yet most are spatially limited to specific districts, use earlier time windows, or emphasize carbon stocks rather than annual GPP dynamics for mangrove ecosystems at the provincial scale.

This study addresses that gap by quantifying the annual dynamics and trends of mangrove GPP in Bali Province for 2019 to 2024 using high-resolution Sentinel-2A surface reflectance data as the primary input. The analysis focuses on two

representative mangrove systems, Taman Nasional Bali Barat and Tahura Ngurah Rai in Benoa Bay, and applies a consistent light-use-efficiency framework to derive annual GPP with attention to interannual variability and site-specific differences. The objective is to provide a province-level, annually resolved baseline of mangrove photosynthetic carbon uptake that can inform coastal conservation, restoration planning, and blue-carbon accounting in Bali.

METHOD

Study area

Bali Province lies at approximately 8°25′23″ South and 115°14′55″ East in the tropical Indo-Pacific. Two representative mangrove systems were analyzed. The first is Tahura Ngurah Rai in Benoa Bay in southern Bali, which is embedded in a periurban coastal setting with active management. The second is Taman Nasional Bali Barat in the northwest, which represents a more protected coastal mosaic (Figure 1). These two systems encompass the largest contiguous mangrove extents in the province and capture a gradient of hydrological and anthropogenic conditions relevant to productivity.

Datasets and analysis

The analysis spans the years 2019 to 2024. The core optical input is Sentinel-2A Surface Reflectance, Harmonized, accessed through Google Earth Engine (collection COPERNICUS/S2_SR_HARMONIZED). Supporting environmental inputs are daily ERA5 reanalysis for surface radiation and basic meteorology (ECMWF/ERA5_DAILY), and MODIS Land Surface Temperature (LST) for canopy thermal conditions (MODIS/061/MOD11A1). All datasets are open access through the Earth Engine platform (https://earthengine.google.com) (Gorelick et al., 2017). A summary of the datasets employed in this study and their respective functions is provided in Table 1.

Preprocessing and annual compositing

All processing was conducted in Google Earth Engine for scalable cloud computation (Badruzzaman et al., 2025; Pflumm et al., 2025; Praticò et al., 2021). Sentinel-2A scenes were filtered to 2019–2024 and clipped to site boundaries that were fixed

Table 1. Data materials and Google Earth Engine (GEF	d) datasets used for quantifying mangrove gross primary	7
productivity (GPP)		

Data material	Dataset name in GEE	GEE Asset ID & Catalog link	Purpose in analysis
Optical imagery	Harmonized Sentinel-2 MSI: MultiSpectral Instrument, Level-2A (SR)	https://developers.google.com/ earth-engine/datasets/catalog/ COPERNICUS_S2_SR_ HARMONIZED	Used to calculate annual median vegetation indices (EVI, LSWI) for deriving the fPAR (fPARchI) and water- stress scalar (Wscalar)
Meteorological data	ERA5-Land Daily Aggregated - ECMWF Climate Reanalysis	https://developers.google.com/earth- engine/datasets/catalog/ECMWF_ ERA5_LAND_DAILY_AGGR	Provided 'surface_solar_radiation_downwards_sum' to calculate annual Photosynthetically Active Radiation (PAR). Provided 'temperature_2m' as a fallback for missing LST data
Land surface temperature	MOD11A2.061 Terra land surface temperature and Emissivity 8-Day Global 1km	https://developers.google.com/earth- engine/datasets/catalog/MODIS_061_ MOD11A2	Used to derive the 'LST_Day_1km' band for calculating the monthly and annual average temperature-scalar (Tscalar)
Study area boundary	User-Defined Geometry (Bali Mangrove)	Research archive of mangrove areas mapped through random forest machine learning	Defines the spatial extent of the analysis. Used to filter all image collections and clip the final GPP output

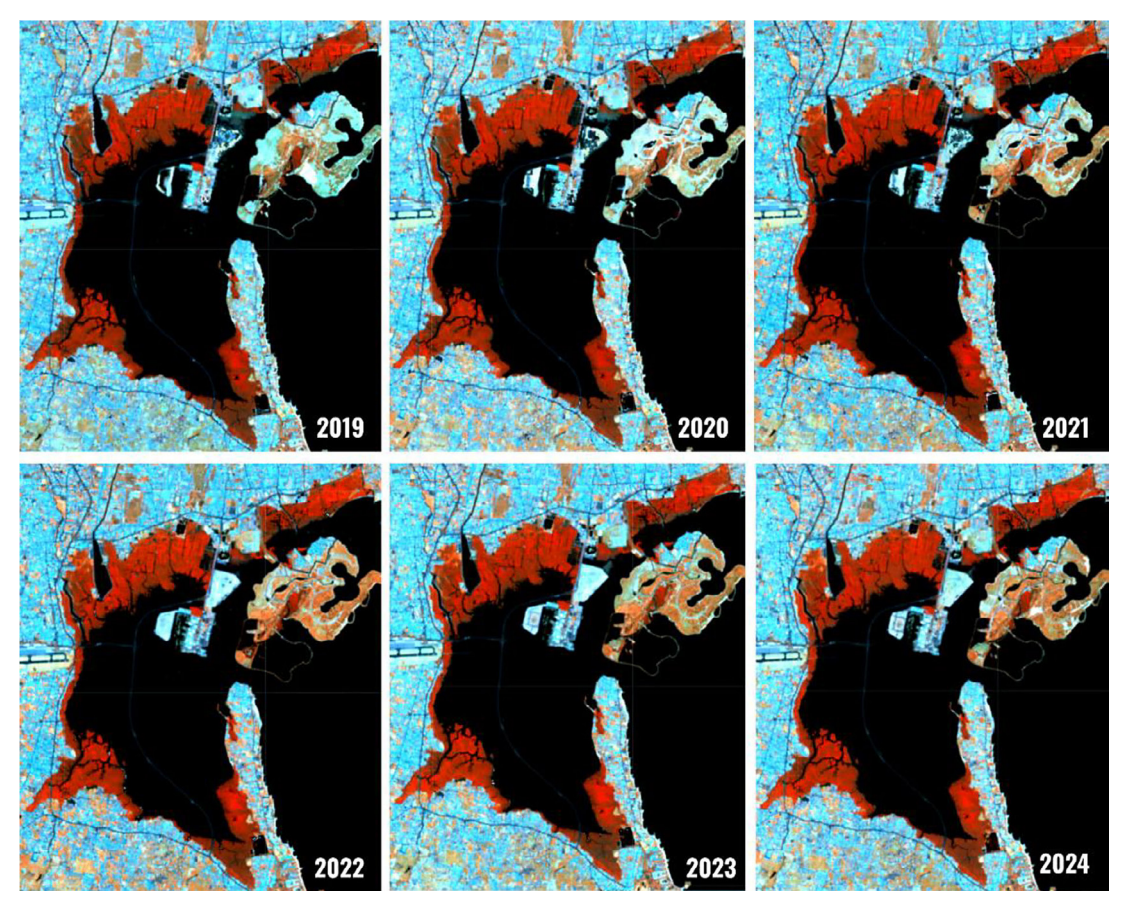


Figure 1. Spatiotemporal overview of the mangrove ecosystem in Tahura Ngurah Rai for 2019 to 2024 (RGB composite: NIR, SWIR1, SWIR2)

for all years. Cloud and cloud-shadow contamination were minimized using the Sentinel-2 cloud probability asset in combination with the QA60 bitmask. Conservative probability thresholds were applied, and remaining artifacts near cloud edges were removed using spectral morphology tests.

Shortwave infrared bands at 20 m were resampled to 10 m to match the native resolution of the blue, red, and near-infrared bands. Annual composites were then generated by aggregating valid observations within each calendar year after quality masking. Sentinel-2A surface reflectance removes the

need for top-of-atmosphere conversions, which ensures radiometric consistency across the record without additional transformations.

Vegetation indices

Vegetation indices sensitive to canopy greenness and water status were computed from surface reflectance. The enhanced vegetation index uses near-infrared, red, and blue bands and is less prone to saturation in dense canopies. The land surface water index uses near-infrared and shortwave infrared bands and is sensitive to canopy water content (Equation 1 and Equation 2).

$$EVI = 2.5 \frac{\rho_{NIR} - \rho_{red}}{\rho_{NIR} + 6 \rho_{red} + + 7.5 \rho_{blue} + 1}$$
(1)

$$LSWI = \frac{\rho_{NIR} - \rho_{SWIR}}{\rho_{NIR} + \rho_{SWIR}}$$
 (2)

where: ρ_{NIR} is Sentinel-2A near-infrared reflectance (Band 8, nominal 842 nm), ρ_{red} is red reflectance (Band 4, nominal 665 nm), ρ_{blue} is blue reflectance (Band 2, nominal 490 nm), and ρ_{SWIR} is shortwave infrared reflectance (Band 11, nominal 1610 nm). All reflectances are dimensionless surface reflectance values.

Fraction of absorbed PAR by chlorophyll

Following the vegetation photosynthesis model (VPM), the fraction of photosynthetically active radiation absorbed by chlorophyll, fPAR_{chl}, was estimated directly from EVI. This approach reduces structural confounding and maintains temporal consistency among years (Equation 3).

$$fPAR_{chl} = EVI$$
 (3)

For sensitivity checks, we also computed a classical NDVI-based relationship for the fraction of absorbed PAR by the canopy (Myneni and Williams, 1994), APAR (Equation 4).

$$fAPAR = 1.1638 \times NDVI - 0.1426$$
 (4)

where: fPAR_{chl} and fPAR are dimensionless fractions, EVI and NDVI are vegetation indices derived from Sentinel-2A surface reflectance, and the primary analyses use fPAR_{ch} = EVI.

Photosynthetically active radiation

Daily downward surface shortwave radiation from ERA5 was converted to photosynthetically active radiation (PAR) and then aggregated to annual totals on the Sentinel-2A grid (Equation 5).

$$PAR = \alpha \times SW_1 \times 10^{-6} \tag{5}$$

where: PAR is photosynthetically active radiation in MJ m⁻² day⁻¹, SW $_{\downarrow}$ is ERA5 daily surface solar radiation downward in J m⁻² day⁻¹, α is the broadband-to-PAR conversion factor, and 10^{-6} converts joules to megajoules.

A value of $\alpha = 0.473$ was used as a standard approximation for the fraction of shortwave energy in the *PAR* waveband. Annual *PAR* was computed by summing daily values within each calendar year.

VPM light-use efficiency model for GPP

Gross primary productivity was estimated using the VPM formulation in energy units. Annual pixel-level GPP is given by the product of lightuse efficiency, the fraction of radiation absorbed by chlorophyll, and the available photosynthetically active radiation (Xiao et al., 2010; Xiao et al., 2004). The computation of GPP is presented in Equation 6.

$$GPP = \varepsilon_g \times fPAR_{chl} \times PAR$$
 (6)

where: GPP is gross primary productivity in g C m⁻² period⁻¹, ε_g is the realized lightuse efficiency in g C MJ⁻¹, fPAR_{chl} is the chlorophyll-absorbed fraction of PAR.

The term ε_g is decomposed into a maximum efficiency and a set of environmental scalars (Equation 7).

$$\varepsilon_g = \varepsilon_0 \times T_{\text{scalar}} \times \times W_{\text{scalar}} \times P_{\text{scalar}}$$
(7)

where: ε_0 is the maximum light-use efficiency for tropical vegetation, T_{scalar} is the temperature scalar, W_{scalar} is the water scalar, and p_{scalar} is the phenology scalar.

A commonly used tropical value was adopted for ε_0 based on the VPM literature, and the same value was used for all years to preserve comparability.

Temperature scalar

The temperature response follows a peaked function using MODIS land surface temperature as the thermal driver (Equation 8).

$$T_{\text{scalar}} = \frac{(T - T_{\text{min}})}{(T - T_{\text{min}})(T - T_{\text{max}})} - (8)$$
$$-(T - T_{\text{opt}})^{2}$$

where: TT is local mean land surface temperature in degrees Celsius, T_{min} is the minimum temperature for photosynthesis, T_{max} is the maximum temperature for photosynthesis, and T_{opt} is the optimum temperature. Tropical values of $T_{min} = 0$ °C, $T_{max} = 48~0$ °C, and $T_{opt} = 28$ °C were used

Water scalar

The canopy moisture constraint uses LSWI normalized by its annual maximum (Equation 9).

$$W_{\text{scalar}} = \frac{1 + LSWI}{1 + LSWI_{max}} \tag{9}$$

where: LSWI is the land surface water index at a given observation and $LSWI_{max}$ is the annual maximum LSWI for the same pixel.

Phenology scalar

Mangrove canopies in the tropics retain photosynthetically active foliage for most of the year. Therefore, a value of $P_{\text{scalar}} = 1$ was adopted for all observations.

Annual integration and site-level aggregation

After computing pixel-level GPP for each valid Sentinel-2A observation date, daily PAR fields were matched by date and location, and annual GPP totals were obtained by temporal integration. Pixels were retained only if the fraction of valid, cloud-free Sentinel-2A observations exceeded a minimum threshold within the year, which reduces the risk of temporal aliasing. Site-level annual GPP was computed as the mean of valid pixels within each mangrove boundary for Tahura Ngurah Rai and Taman Nasional Bali Barat. Companion datacoverage layers were stored to document observation density.

Quality control and sensitivity checks

Quality control combined conservative cloud masking, spectral edge removal, and robust statistics during compositing to limit the influence of outliers. Sensitivity checks evaluated the stability of results to the choice of $fPAR_{chl}$ by comparing EVI-based $fPAR_{chl}$ with the NDVI-based fAPAR formulation. Additional checks summarized the temporal behavior of the environmental scalars T_{scalar} , W_{scalar} , and P_{scalar} to ensure that no single factor produced unrealistic interannual swings.

RESULTS

Sentinel-2A annual composites and spatial context

Annual Sentinel-2A surface reflectance composites for 2019–2024 show stable near-infrared signals over core mangrove stands, with stronger shortwave-infrared variability along tidal margins. In Tahura Ngurah Rai, the coastal mosaic that includes channels, embankments, and built areas is clearly resolved, while contiguous canopy blocks on the western and southern sectors display consistent near-infrared reflectance through time. These patterns are visible in the annual three-band render that combines near-infrared, shortwave-infrared 1, and shortwave-infrared 2. As seen in Figure 1, spatial consistency in core stands contrasts with dynamic moisture signals around channels and embankments. In Taman Nasional Bali Barat, core stands exhibit steady near-infrared reflectance across years, and changes are more apparent along edges that interact with bays and tidal flats, as illustrated in Figure 2. These spatial differences anticipate where environmental scalars are most likely to modulate annual GPP.

Spatial distribution of annual GPP

Maps of annual GPP derived from the VPM framework reveal a coherent spatial hierarchy of productivity within each ecosystem. In Tahura Ngurah Rai, high values cluster in the protected blocks with dense canopy, while lower values occur near mixed pixels that include open water, muddy substrates, or built structures. As seen in Figure 3, these gradients are stable across years but modulated in magnitude by interannual

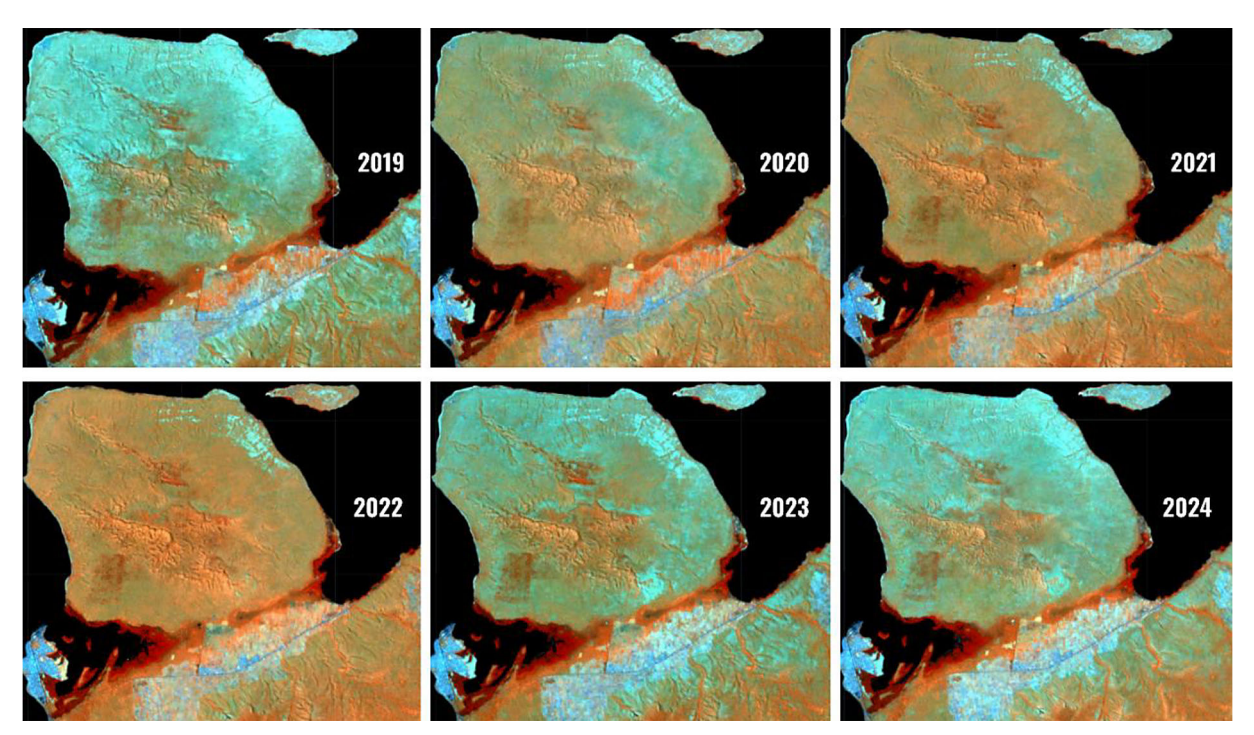


Figure 2. Spatiotemporal overview of the mangrove ecosystem in Taman Nasional Bali Barat for 2019 to 2024 (RGB composite: NIR, SWIR1, SWIR2)

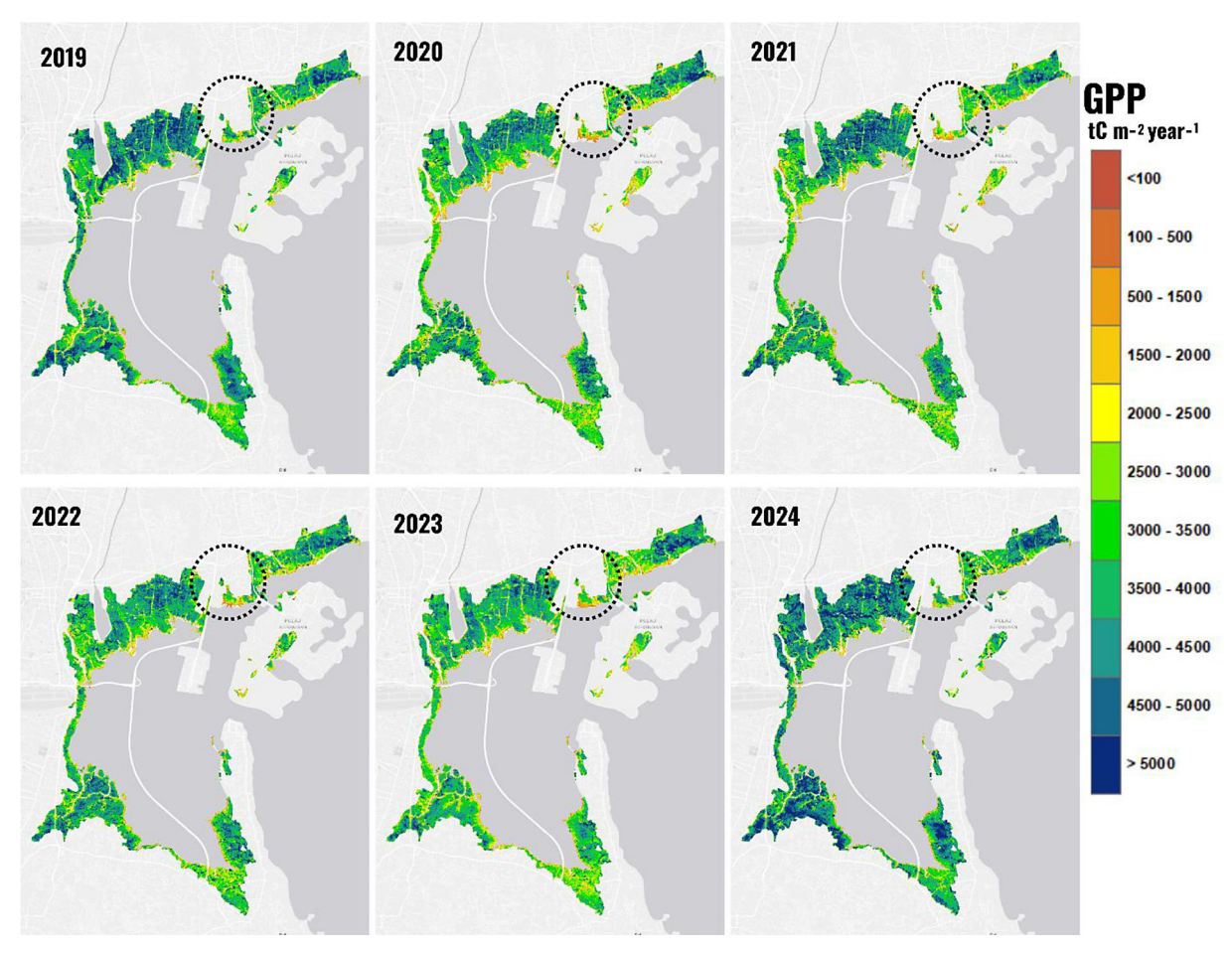


Figure 3. Spatial distribution of gross primary productivity (GPP) in the Tahura Ngurah Rai mangrove ecosystem from 2019 to 2024. The dotted circle highlights a persistent area of low GPP (yellow-orange colours), while dark blue indicates high GPP values

changes in moisture and radiation. In Taman Nasional Bali Barat, as shown in Figure 4, peak values align with the interior of mature stands, whereas margins that experience greater tidal exchange show lower and more variable GPP. The spatial configuration indicates that fPAR_{chl} tends to be high and steady in interior canopies, while the water scalar varies more strongly in edge environments where shortwave-infrared indices capture moisture dynamics.

Zonal analysis across ecosystems

The zonal statistics clarify how spatial structure translates into annual productivity differences. Across zones, the highest mean GPP during 2019–2024 occurs in Zone VI with 4.386 g C m⁻² yr⁻¹, followed by Zone VII with 3.971 g C m⁻² yr⁻¹, Zone IV with 3.846 g C m⁻² yr⁻¹, and Zone VIII with 3.774 g C m⁻² yr⁻¹. Intermediate means are found in Zone I with 3.629 g C m⁻² yr⁻¹ and Zone II with 3.553 g C m⁻² yr⁻¹, while the lowest occurs in Zone V with 2.756 g C m⁻² yr⁻¹. Variability is lowest in Zone IV, where the coefficient of variation is 1.6%, indicating exceptional yearto-year stability. Variability is highest in Zone V, where the coefficient of variation reaches 12.8%, consistent with environmental pressure and spectral mixing at the edge of landfill-affected areas.

As seen in Figure 5, the zone layout spans both ecosystems and preserves these contrasts for consistent interannual comparison.

When zones are separated by ecosystem, Zones I and II represent Taman Nasional Bali Barat. Zone I shows a gentle decline from 3.666 g C m⁻² yr⁻¹ in 2019 to 3.522 g C m⁻² yr⁻¹ in 2024, equivalent to a linear decrease of 28 g C m⁻² yr⁻² and a net change of -3.9%. The pattern suggests reduced canopy moisture in some shoreline segments, leading to lower water scalars. Zone II increases from 3.305 g C m⁻² yr⁻¹ to 3.966 g C m⁻² yr⁻¹, a rise of about 20%, which is consistent with modest gains in $fPAR_{chl}$ in interior stands and more favorable moisture conditions along edges. Zones III through VIII correspond to Tahura Ngurah Rai. Zone VI is consistently the highest across all years with the sequence 4,458, 4.312, 4.221, 4.188, 4.658, and 4.481 g C m⁻² yr⁻¹, reflecting a protected block with dense canopy where EVI and fPAR_{chl} remain high and the water scalar remains favorable. Zone IV also maintains high and stable values, which aligns with minimal edge disturbance and a mature canopy structure. Figure 6 summarizes the zonal time series and highlights the contrast between stable interior zones and more variable edge zones.

Zone V, located around the Suwung landfill, has the lowest mean and the highest variability.

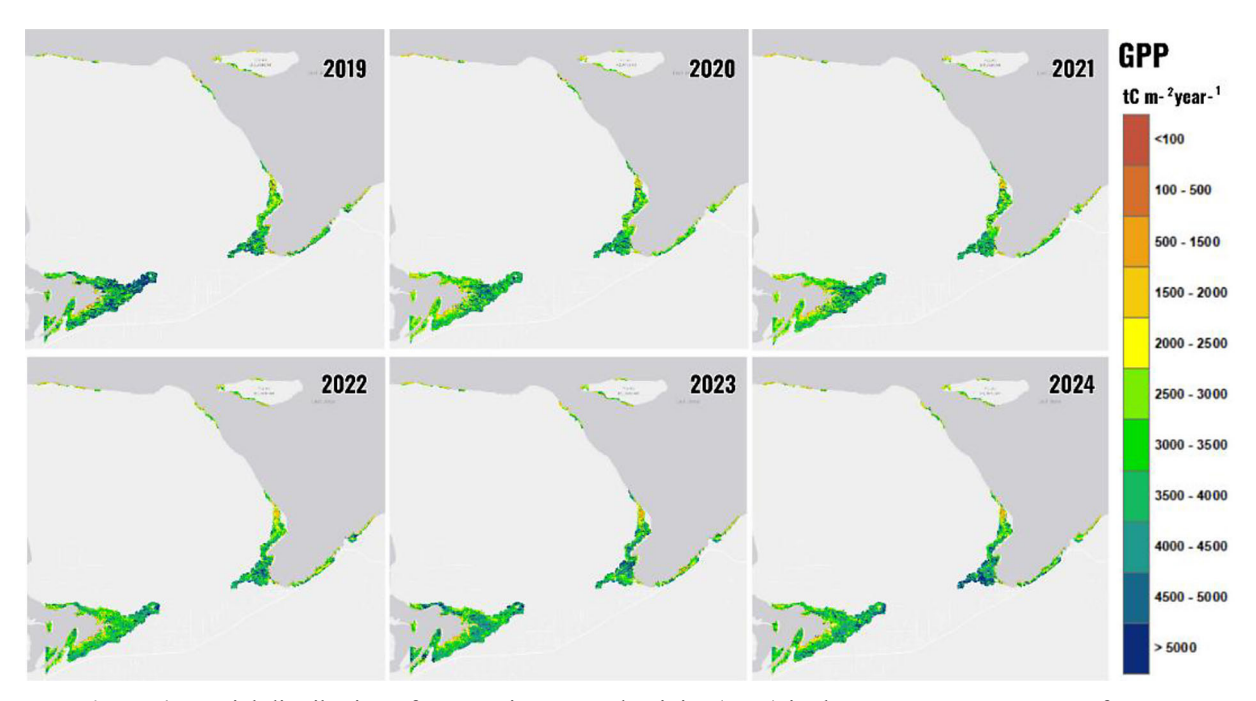


Figure 4. Spatial distribution of gross primary productivity (GPP) in the mangrove ecosystem of Taman Nasional Bali Barat from 2019 to 2024. Yellow-orange colours indicate areas of low GPP, while dark blue indicates high GPP values

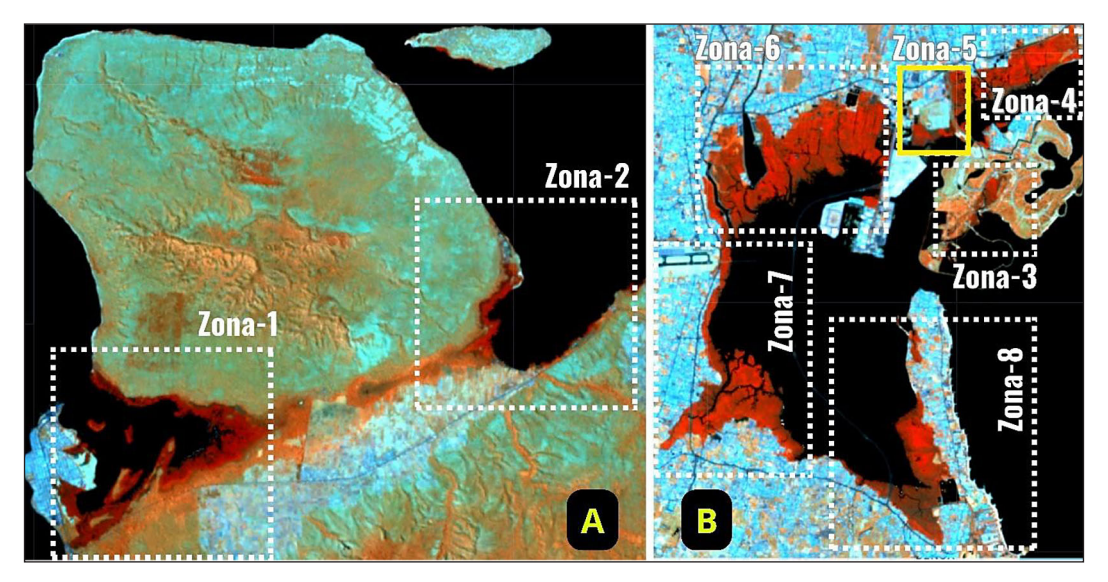


Figure 5. Layout of the GPP sampling zones in Taman Nasional Bali Barat (A) and Tahura Ngurah Rai (B). These zones are used as the basis for comparing GPP time-series based on pixel values

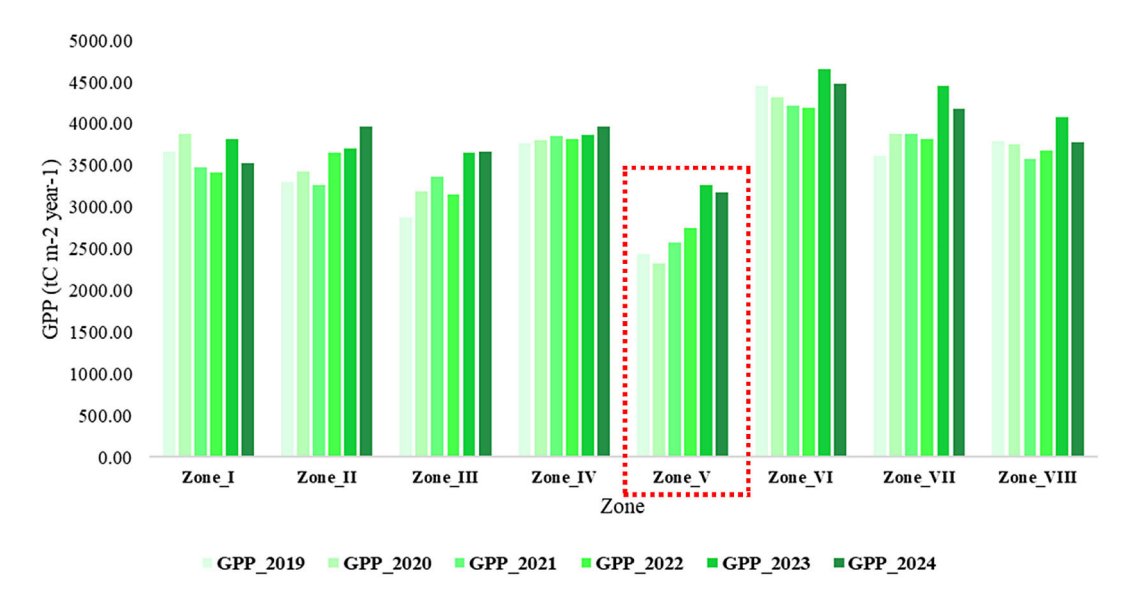


Figure 6. Annual gross primary productivity (GPP) by sampling zone from 2019 to 2024. Zone V (highlighted) consistently shows significantly lower GPP values compared to all other zones, making it a high priority for targeted mangrove management and restoration

Lower EVI and LSWI in mixed pixels that include open water or exposed substrate reduce *f*PAR_{chl} and the water scalar, which depresses GPP. Even so, Zone V exhibits a partial recovery up to 2023, increasing from 2.444 g C m⁻² yr⁻¹ to 3.264 g C m⁻² yr⁻¹, followed by a small decline in 2024. Zone VII increases strongly through 2023 and remains high in 2024, whereas Zone VIII remains in the middle to upper range with a peak in 2023. These behaviors confirm that differences among zones are primarily governed by canopy density recorded by EVI and by moisture status recorded by LSWI, with additional modulation from

interannual changes in photosynthetically active radiation and temperature.

Interannual dynamics 2019–2024

At the ecosystem scale, both sites show rising GPP across the study period with a shared maximum in 2023 and a modest correction in 2024. The mean annual GPP for 2019–2024 is 3.591 g C m⁻² yr⁻¹ in Taman Nasional Bali Barat and 3.675 g C m⁻² yr⁻¹ in Tahura Ngurah Rai. Taman Nasional Bali Barat increases by 7.4%, from 3.486 to 3.744 g C m⁻² yr⁻¹. Tahura Ngurah Rai increases by

11.0%, from 3.490 to 3.873 g C m⁻² yr⁻¹. Peak values occur in 2023 at 3.758 g C m⁻² yr⁻¹ for Taman Nasional Bali Barat and 3.996 g C m⁻² yr⁻¹ for Tahura Ngurah Rai. These trajectories are displayed in Figure 7. The province-level signal shows a similar pattern when the two sites are averaged, indicating that the 2023 conditions were favourable for canopy photosynthesis, followed by slightly lower but still elevated values in 2024 relative to 2019.

Linkage to blue-carbon function and management urgency

The observed increases in annual GPP indicate greater assimilation of atmospheric carbon into mangrove biomass during 2019-2024. In the context of blue-carbon ecosystems, higher GPP is a necessary condition for strengthening the carbon sink, because it provides the photosynthetic input that supports biomass growth and organic matter accumulation. These results therefore carry strong management relevance. First, the positive trajectory implies that protection and targeted restoration can maintain or enhance productivity, particularly in interior zones with high fPAR_{chl} and favorable moisture. Second, zones that show lower means and higher variability, such as the area around the Suwung landfill, represent opportunities for focused interventions that stabilize water status and reduce spectral mixing with non-vegetated surfaces. Third, the shared peak in 2023 and the slight decline in 2024 underscore the sensitivity of productivity to interannual climate variability, reinforcing the need for continuous monitoring to secure gains under changing environmental conditions. Read together, the spatial structure, the zonal contrasts, and the interannual rise highlight the urgent and crucial role of Bali's mangroves in blue-carbon strategies for emission reduction and climate resilience at the provincial scale.

DISCUSSION

This study presents the first province-wide, annually resolved assessment of mangrove gross primary productivity in Bali using high-resolution Sentinel-2A observations for 2019 to 2024. The results show consistent increases in annual GPP at Taman Nasional Bali Barat and Tahura Ngurah Rai, peaking in 2023, with only a modest decline in 2024. Because GPP sets the upper bound for the blue-carbon sink, these gains indicate greater photosynthetic assimilation of atmospheric carbon during the study period and therefore strengthen the case for mangrove protection and targeted rehabilitation as part of Bali's climate mitigation strategy. The spatial patterns reported in Figures 1 to 6 and the time-series trajectories in Figure 7 together demonstrate that interior, wellmanaged stands maintain high fPAR_{chl} and favorable moisture conditions, while edge zones near mixed substrates and infrastructure show lower means and higher variability. This spatial contrast

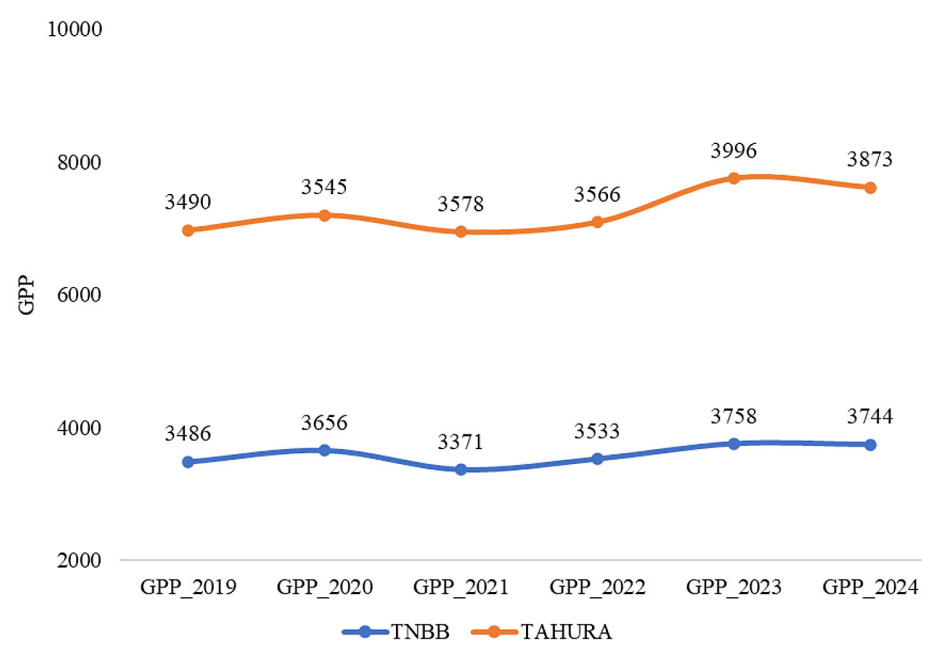


Figure 7. Mean gross primary productivity (GPP) of mangrove ecosystems in Bali Province, 2019 to 2024

creates clear priorities for management: protect stable interior blocks to preserve high productivity and focus interventions on edge zones to improve canopy continuity and water status.

Globally, mangroves are among the most productive coastal ecosystems and contribute substantially to blue-carbon fluxes (Franco et al., 2025; Ouyang et al., 2024; Zhang et al., 2024). Reviews indicate that productivity varies with salinity, rainfall, tidal flooding, light, canopy age, nutrient availability, disturbance history, and geomorphic setting, and that global mangrove GPP has increased since 2001 with continued increases likely under rising atmospheric CO2 (Alongi, 2025). Against this backdrop, Bali's positive GPP trend aligns with international evidence that wellprotected or recovering mangroves can sustain or improve photosynthetic capacity. The 2023 maximum observed in both sites is consistent with years that combine adequate radiation with thermal and moisture regimes within mangrove physiological optima. The small decline in 2024 suggests sensitivity to interannual climate variability, which underscores the value of continuous monitoring.

A central contribution of this work is the use of 10 m Sentinel-2A surface reflectance to derive annual GPP via a light-use-efficiency framework. Much of the earlier literature has relied on coarser products for regional GPP estimates. For example, studies that use MODIS GPP at kilometre to 500 m resolution can reveal provincial or national signals but cannot resolve the sharp gradients that characterize mangrove mosaics near channels, embankments, and mixed intertidal substrates (Menefee et al., 2023; Muñoz-Albiter et al., 2024; Wang et al., 2024; Zhang et al., 2023). Coarse pixels blend vegetation, water, and built surfaces, which suppresses peak values in dense stands and exaggerates variability at edges. By contrast, our Sentinel-2A approach captures fine-scale structure in fPAR_{chl} and LSWI, allowing robust differentiation between interior and edge zones and producing zonal statistics that are stable where canopies are continuous and variable where spectral mixing occurs. This resolution advantage matches recent advances in mangrove GPP modeling that integrate Sentinel-2 reflectance, refined fAPAR estimation, and machine learning to quantify environmental drivers and detect spatial heterogeneity that coarse data miss (Zheng et al., 2025; Zheng and Takeuchi, 2022).

Comparisons with work outside Indonesia help situate Bali's findings. On Hainan Island, optimized ensembles combining Sentinel-2-derived fAPAR with an MVP-LUE model reported increasing annual GPP and strong control of productivity by fAPAR, with seasonal peaks during the transition from dry to rainy periods (Zheng et al., 2025). This seasonal sensitivity is consistent with our interannual signals in Figure 7, where favorable radiation and moisture conditions promote higher GPP. In northwestern Mexico, seasonality associated with the North American Monsoon produced GPP maxima before the monsoon, while temperature and vapor pressure deficit became stronger drivers during and after the monsoon (Muñoz-Albiter et al., 2024). These results echo the role of the temperature and water scalars in our model. They also point to the need for local measurements of vapor pressure deficit and inundation timing to refine scalar behaviour in coastal settings. High-resolution retrievals are essential in mangroves because small hydrological shifts can create large productivity differences over tens of meters, a scale that coarse sensors cannot resolve. Studies that used high-resolution optical sensors or downscaled drivers have shown improved agreement with flux observations and better attribution of environmental controls, further supporting the approach taken here (Lele et al., 2021).

Extreme events add another layer of variability and risk to blue-carbon services. Tropical cyclones and storm surges can reduce photosynthetic area and alter physiological rates, with recovery times that vary by community composition, soil conditions, tree size distributions, and distance to storm tracks and shorelines (Wu et al., 2023; Zou et al., 2025). Although Bali is less exposed to intense cyclones than some subtropical islands, episodic storm surges and compound flooding events can still affect canopy condition and sediment dynamics. The shared peak in 2023 followed by a slight decline in 2024 could reflect interannual climate anomalies that affect radiation, humidity, and inundation frequency. Integrating tide-aware compositing and hydrodynamic indicators in future remote-sensing workflows should improve attribution of such year-to-year changes.

From a blue-carbon perspective, the increases in GPP observed here are urgent and policy-relevant (Wu et al., 2023; Zou et al., 2025). GPP provides the photosynthetic input to net ecosystem production, which, after accounting for respiration and lateral exports, underpins long-term carbon storage in biomass and sediments (Alwis et al., 2025; Hurd et al., 2022; Lamont et al., 2020).

The spatial concentration of high GPP in interior zones implies that maintaining hydrological connectivity, minimizing edge disturbance, and preventing conversion around these blocks will sustain annual carbon assimilation. Conversely, lower and more variable GPP in edge zones near mixed land uses highlights where restoration can deliver immediate gains by reducing spectral mixing with non-vegetated surfaces, improving water management, and promoting canopy closure. Because Bali's coastal development pressures are ongoing, the demonstrated productivity gains are not guaranteed. They require continued protection and fine-scale management, especially where infrastructure and landfill activities interact with mangrove margins.

The urgency of protecting these high-GPP ecosystems is therefore two-fold, extending beyond carbon mitigation to include critical climate adaptation. First, the high photosynthetic assimilation (GPP) documented in this study is the primary mechanism for carbon sequestration. This function provides an essential, quantifiable counterbalance to the significant regional greenhouse gas emissions linked to Bali's vital tourism sector (Saifulloh, et al., 2025; Sunarta and Saifulloh, 2022b, 2022a). Second, and of more immediate local importance, these mangrove stands function as indispensable natural infrastructure. Their complex root structures dissipate wave energy, providing a physical buffer against the coastal flooding that threatens the region (Trigunasih and Saifulloh, 2022). Furthermore, their ability to trap sediment and build soil (a process known as vertical accretion) is a critical natural defense against the dual threats of sea-level rise and the alarming rates of land subsidence (Saifulloh et al., 2025), the latter often exacerbated by groundwater extraction in tourism-heavy areas. This multi-faceted crisis, driven by development and overtourism (Sunarta et al., 2025), highlights the non-negotiable value of preserving all green open spaces. The coastal mangroves, as demonstrated by their GPP, provide a direct carbon-sink and a physical resilience service, which is complemented by urban terrestrial forests that offer parallel benefits (e.g., mitigating the urban heat island effect) (Sudarma et al., 2024; Sunarta et al., 2022). Therefore, protecting these ecosystems is a core strategy for mitigating the severe, interconnected environmental degradation facing the province.

This study has limitations that future work should address. Field validation of GPP in tidal

mangroves remains scarce, eddy-covariance towers are uncommon, and partitioning net exchange into GPP and ecosystem respiration under tidal influence is still challenging. Light-use-efficiency parameters were held constant across years for comparability, yet site-level differences in species composition, nutrient status, and salinity may shift optimal efficiency. The temperature scalar uses MODIS land surface temperature as a proxy for canopy thermal conditions that can diverge from air or leaf temperature in some seasons, and the water scalar based on LSWI and its annual maximum can be affected by subpixel water, bright adjacency, and tide timing. Despite conservative cloud screening and compositing, residual artifacts and limited clear scenes in some months introduce additional uncertainty into annual integration.

Looking ahead, several practical steps can narrow these uncertainties and strengthen comparability with field observations. The first is to install at least one flux tower in each ecosystem and apply tidal-aware partitioning to derive GPP from continuous net ecosystem exchange. The second is to conduct tide-synchronized field campaigns that pair leaf gas exchange, chlorophyll content, and leaf area index with high-resolution drone multispectral or hyperspectral imagery, creating a link from leaf physiology to canopy signals. The third is to integrate solar-induced chlorophyll fluorescence and lidar-derived canopy structure, where available, to refine estimates of fPAR chl and light interception. The fourth is to incorporate salinity, water level, and porewater metrics so the environmental scalars represent hydrological controls more explicitly than temperature and optical moisture alone. The fifth is to apply tide-aware compositing and adjacency correction in Sentinel-2 processing to reduce edge contamination in narrow coastal strips. Together, these focused improvements will reduce uncertainty and directly support the management priorities outlined in the Conclusion, namely protecting high-performing interior canopies and restoring vulnerable edges to sustain Bali's blue-carbon benefits.

CONCLUSIONS

This study provides the first province-wide, annually resolved picture of mangrove gross primary productivity in Bali using Sentinel-2A for 2019 to 2024. Productivity increased over time and peaked in 2023, with interior, well-managed

stands consistently higher than edge zones near mixed substrates. These patterns indicate a strengthening photosynthetic carbon uptake that supports Bali's blue-carbon objectives and identifies clear priorities for action: maintain protection of interior canopies and restore edges through improved hydrology and canopy continuity.

The Sentinel-2A approach resolves fine-scale heterogeneity that coarser products cannot, making the results directly useful for targeting management and for updating provincial inventories. Remaining uncertainty is mainly due to limited field validation of GPP in tidal forests. Future work should couple high-resolution monitoring with flux towers and tide-synchronized field measurements to reduce uncertainty and to sustain the blue-carbon benefits of Bali's mangroves.

Acknowledgements

We thank the anonymous reviewers for their constructive comments and suggestions that improved this manuscript. We also acknowledge the Udayana University Research and Community Service Institute for facilitation and support throughout the study. This work was supported by the DIPA PNBP Universitas Udayana for Fiscal Year 2025 under the Research Implementation Assignment Agreement Letter No. B/229.195/UN14.4.A/PT.01.03/2025, dated April 28, 2025.

REFERENCES

- 1. Alongi, D. M. (2025). Global meta-analysis of mangrove primary production: implications for carbon cycling in mangrove and other coastal ecosystems. *Forests*, 16(5), 747.
- Alwis, R., Pawuluwage, S. M., Bellanthudawa, B. K. A., Perera, I., Nawalage, N., Amarathunga, A. A. D., Halwatura, D. (2025). The role of small-scale mangrove conservation forests in enhancing above-and below-ground carbon sequestration: A critical measure of blue carbon stock for climate change mitigation. Regional Studies in Marine Science, 104546.
- As-syakur, A. R., Setiawati, M. D., Mukaromah, L., Osawa, T., Adnyana, I. W. S., Sunarta, I. N. (2023). Growing urban tourism activities while increasing vegetation ecosystem service under land use changes pressure: a case study of Sanur, Bali, Indonesia. In *Springer Geography*. https://doi. org/10.1007/978-3-031-24767-5_29
- 4. Badan Pusat Statistik. (2024). Central Bureau of Statistics Bali. *BPS*, *1101001*.

- Badruzzaman, A., Wulandari, P., Sainal, S., Ashley, M., Jobling, S., Austen, M. C., Praptiwi, R. A. (2025). Satellite imagery pre-processing and feature extraction for the mapping of coastal ecosystems using Google Earth Engine: A workflow for practitioners. *MethodsX*, 103516.
- Donato, D. C., Kauffman, J. B., Murdiyarso, D., Kurnianto, S., Stidham, M., Kanninen, M. (2011). Mangroves among the most carbon-rich forests in the tropics. *Nature Geoscience*, 4(5), 293–297. https://doi.org/10.1038/ngeo1123
- Franco, J. N., Sainz Meyer, H., Babe, Ó., Martins, M., Reis, B., Sanchez-Gallego, Á., Lemos, M. F. L., Dolbeth, M., Sousa-Pinto, I., Arenas, F. (2025). Potential blue carbon in the fringe of Southern European Kelp forests. *Scientific Reports*, 15(1), 29573.
- 8. Gorelick, N., Hancher, M., Dixon, M., Ilyushchenko, S., Thau, D., Moore, R. (2017). Google Earth Engine: Planetary-scale geospatial analysis for everyone. *Remote Sensing of Environment*, 202. https://doi.org/10.1016/j.rse.2017.06.031
- Government of Indonesia. (2022). Enhanced Nationally Determined Contribution Republic of Indonesia 2022.
- 10. Hidayah, Z., Utama, R. Y. S., As-Syakur, A. R., Rachman, H. A., Wiyanto, D. B. (2024). Mapping mangrove above ground carbon stock of benoa bay bali using sentinel-1 satellite imagery. *IOP Conference Series: Earth and Environmental Science*, 1298(1). https://doi.org/10.1088/1755-1315/1298/1/012013
- 11. Hurd, C. L., Law, C. S., Bach, L. T., Britton, D., Hovenden, M., Paine, E. R., Raven, J. A., Tamsitt, V., Boyd, P. W. (2022). Forensic carbon accounting: Assessing the role of seaweeds for carbon sequestration. *Journal of Phycology*, 58(3), 347–363.
- Lamont, K., Saintilan, N., Kelleway, J. J., Mazumder, D., Zawadzki, A. (2020). Thirty-year repeat measures of mangrove above-and below-ground biomass reveals unexpectedly high carbon sequestration. *Ecosystems*, 23(2), 370–382.
- 13. Lele, N., Kripa, M. K., Panda, M., Das, S. K., Nivas, A. H., Divakaran, N., Naik-Gaonkar, S., Sawant, A., Pattnaik, A. K., Samal, R. N. (2021). Seasonal variation in photosynthetic rates and satellite-based GPP estimation over mangrove forest. *Environmental Monitoring and Assessment*, 193(2), 61.
- 14. McLeod, E., Chmura, G. L., Bouillon, S., Salm, R., Björk, M., Duarte, C. M., Lovelock, C. E., Schlesinger, W. H., Silliman, B. R. (2011). A blue-print for blue carbon: Toward an improved understanding of the role of vegetated coastal habitats in sequestering CO₂. In Frontiers in Ecology and the Environment 9(10). https://doi.org/10.1890/110004
- 15. Menefee, D., Lee, T. O., Flynn, K. C., Chen, J., Abraha, M., Baker, J., Suyker, A. (2023). Machine learning algorithms improve MODIS GPP estimates

- in United States croplands. Frontiers in Remote Sensing, 4, 1240895.
- 16. Ministry of Environment and Foresty as National Focal Point UNFCCC. (2022). Enhanced NDC: Komitmen Indonesia Untuk Makin Berkontribusi Dalam Menjaga Suhu Global. Press Release Number SP.271/HUMAS/PPIP/HMS.3/9/2022.
- 17. Muñoz-Albiter, M. E., Velázquez-Rodríguez, A. S., Sanchez-Mejia, Z. M. (2024). Seasonal gross primary production in response to environmental drivers from arid mangroves in the Gulf of California. *Remote Sensing Applications: Society and Environment*, 33(October 2022). https://doi.org/10.1016/j. rsase.2023.101096
- 18. Myneni, R. B., Williams, D. L. (1994). On the relationship between FAPAR and NDVI. *Remote Sensing of Environment*, 49(3). https://doi.org/10.1016/0034-4257(94)90016-7
- 19. Nuarsa, I. W. (2016). Peranan teknologi remote sensing dan GIS dalam pengelolaan sumberdaya alam. *Jurnal Internasional*, 8(2).
- Nuarsa, I. W., Wayan, I., Adnyana, S., Rahman As-Syakur, A. (2015). Pemetaan daerah rawan kekeringan di Bali-Nusa Tenggara dan hubungannya dengan ENSO menggunakan aplikasi data penginderaan Jauh. *Jurnal Bumi Lestari*, 15(1)(Pebruari).
- 21. Nuarsa, W., As-Syakur, A. R., Gunadi, I. G. A., Sukewijaya, I. M. (2018). Changes in gross primary production (GPP) over the past two decades due to land use conversion in a tourism city. *ISPRS International Journal of Geo-Information*, 7(2). https://doi.org/10.3390/ijgi7020057
- 22. Ouyang, X., Guo, F., Lee, S. Y. (2024). Multiple drivers for carbon stocks and fluxes in different types of mangroves. *Science of the Total Environment*, 906, 167511.
- 23. Pflumm, L., Kang, H., Wilting, A., Niedballa, J. (2025). GEE-PICX: generating cloud-free Sentinel-2 and Landsat image composites and spectral indices for custom areas and time frames—a Google Earth Engine web application. *Ecography*, 2025(5), e07385.
- 24. Praticò, S., Solano, F., Di Fazio, S., Modica, G. (2021). Machine learning classification of mediterranean forest habitats in google earth engine based on seasonal sentinel-2 time-series and input image composition optimisation. *Remote Sensing*, *13*(4), 586.
- 25. Running, S. W., Nemani, R. R., Heinsch, F. A., Zhao, M., Reeves, M., Hashimoto, H. (2004). A continuous satellite-derived measure of global terrestrial primary production. In *BioScience 54*(6). https://doi.org/10.1641/0006-3568(2004)054[0547:ACS MOG]2.0.CO;2
- Saifulloh, M., Santosa, I. G. N., Sunarta, I. N., Ambarawati, I. G. A. A., Sudarma, I. M., As-syakur, A. R. (2025). Mapping GHG emission vulnerability

- using convolutional autoencoder and multi-sensor satellite in Bali, Indonesia. *Geography, Environment, Sustainability*, 18(3), 135–144.
- 27. Saifulloh, M., Sunarta, I. N., Baiquni, M., Trigunasih, N. M., Adikampana, I. (2025). Linking annual land subsidence to built-up density across coastal tourism zones via Sentinel-1 differential interferometric synthetic aperture radar. *Ecological Engineering & Environmental Technology (EEET)*, 26(9).
- 28. Sri Rahayu Romadhoni, L., As-Syakur, A. R., Hidayah, Z., Budi Wiyanto, D., Safitri, R., Yusuf Satriyana Utama, R., Made Sara Wijana, I., Putra Anugrah, A., Made Oka Guna Antara, I. (2022). Annual characteristics of gross primary productivity (GPP) in mangrove forest during 2016–2020 as revealed by Sentinel-2 remote sensing imagery. IOP Conference Series: Earth and Environmental Science, 1016(1). https://doi.org/10.1088/1755-1315/1016/1/012051
- 29. Suardana, A. A. M. A. P., Anggraini, N., Nandika, M. R., Aziz, K., As-Syakur, A. R., Ulfa, A., Wijaya, A. D., Prasetio, W., Winarso, G., Dimyati, R. D. (2023). Estimation and mapping above-ground mangrove carbon stock using Sentinel-2 data derived vegetation indices in Benoa Bay of Bali Province, Indonesia. *Forest and Society*, 7(1). https://doi.org/10.24259/fs.v7i1.22062
- Sudarma, I., Saifulloh, M., Diara, I. W., As-Syakur, A. (2024). Carbon Stocks dynamics of urban green space ecosystems using time-series vegetation indices. *Ecological Engineering & Environmental Technology (EEET)*, 25(9).
- 31. Sugiana, I. P., Prartono, T., Rastina, Koropitan, A. F. (2024). Ecosystem carbon stock and annual sequestration rate from three genera-dominated mangrove zones in Benoa Bay, Bali, Indonesia. *Biodiversitas*, 25(1). https://doi.org/10.13057/biodiv/d250133
- 32. Sunarta, I. N., Saifulloh, M. (2022a). Coastal tourism: impact for built-up area growth and correlation to vegetation and water indices derived from Sentinel-2 remote sensing imagery. *Geojournal of Tourism and Geosites*, 41(2). https://doi.org/10.30892/gtg.41223-857
- 33. Sunarta, I. N., Saifulloh, M. (2022b). Spatial variation Of NO₂ levels during the Covid-19 pandemic in the Bali tourism area. *Geographia Technica*, 17(1). https://doi.org/10.21163/GT_2022.171.11
- 34. Sunarta, I. N., Suyarto, R., Saifulloh, M., Wiyanti, W., Susila, K. D., Kusumadewi, L. G. L. (2022). Surface urban heat island (SUHI) phenomenon in Bali and Lombok tourism areas based on remote sensing. *Journal of Southwest Jiaotong University*, *57*(4). https://doi.org/10.35741/issn.0258-2724.57.4.44
- Sunarta, N., Arida, I., Trigunasih, N. M., Michele, K., Saifulloh, M. (2025). Overtourism triggered built-up expansion over a decade in Canggu, Bali. Ecological Engineering & Environmental Technology (EEET), 26(10).

- 36. Trigunasih, N. M., Saifulloh, M. (2022). The investigating water infiltration conditions caused by annual urban flooding using integrated remote sensing and geographic information systems. *Journal of Environmental Management & Tourism*, 13(5), 1467–1480.
- 37. Wang, S., Zhang, X., Hou, L., Sun, J., Xu, M. (2024). Estimating global gross primary production using an improved MODIS leaf area index dataset. *Remote Sensing*, *16*(19), 3731.
- 38. Wu, L., Guo, E., An, Y., Xiong, Q., Shi, X., Zhang, X., Sun, Z. (2023). Evaluating the losses and recovery of GPP in the subtropical mangrove forest directly attacked by tropical cyclone: case study in Hainan Island. *Remote Sensing*, *15*(8), 2094.
- 39. Xiao, J., Zhuang, Q., Law, B. E., Chen, J., Baldocchi, D. D., Cook, D. R., Oren, R., Richardson, A. D., Wharton, S., Ma, S., Martin, T. A., Verma, S. B., Suyker, A. E., Scott, R. L., Monson, R. K., Litvak, M., Hollinger, D. Y., Sun, G., Davis, K. J., ... Wofsy, S. C. (2010). A continuous measure of gross primary production for the conterminous United States derived from MODIS and AmeriFlux data. *Remote Sensing of Environment*, *114*(3). https://doi.org/10.1016/j.rse.2009.10.013
- 40. Xiao, X., Hollinger, D., Aber, J., Goltz, M., Davidson, E. A., Zhang, Q., Moore, B. (2004). Satellite-based modeling of gross primary production in an evergreen needleleaf forest. *Remote Sensing of Environment*, 89(4). https://doi.org/10.1016/j.rse.2003.11.008

- 41. Zhang, J., Gan, S., Yang, P., Zhou, J., Huang, X., Chen, H., He, H., Saintilan, N., Sanders, C. J., Wang, F. (2024). A global assessment of mangrove soil organic carbon sources and implications for blue carbon credit. *Nature Communications*, *15*(1), 8994.
- 42. Zhang, Y., Hu, Z., Wang, J., Gao, X., Yang, C., Yang, F., Wu, G. (2023). Temporal upscaling of MODIS instantaneous FAPAR improves forest gross primary productivity (GPP) simulation. *International Journal of Applied Earth Observation and Geoinformation*, 121, 103360.
- 43. Zhao, M., Heinsch, F. A., Nemani, R. R., Running, S. W. (2005). Improvements of the MODIS terrestrial gross and net primary production global data set. *Remote Sensing of Environment*, *95*(2). https://doi.org/10.1016/j.rse.2004.12.011
- 44. Zheng, Y., Shi, X., Lu, R., Guo, S., Zhang, X., Nie, T., Wang, P., Sun, Z. (2025). Spatiotemporal dynamics and environmental drivers of gross primary productivity in mangrove ecosystems of Hainan Island. *Regional Studies in Marine Science*, 104454.
- 45. Zheng, Y., Takeuchi, W. (2022). Estimating mangrove forest gross primary production by quantifying environmental stressors in the coastal area. *Scientific Reports*, *12*(1), 2238.
- 46. Zou, H., Zhu, J., Tian, Z., Chen, Z., Xue, Z., Li, W. (2025). Response mechanism of carbon fluxes in restored and natural mangrove ecosystems under the effects of storm surges. *Forests*, 16(7), 1115.